

Experiment on Instability of Horizontal Rotor System Partially Filled with Small Amounts of Fluid^{*}

WANG Yan-kai, WANG Tong, LIAO Ming-fu, WANG Xin

(School of Power and Energy, Northwestern Polytechnical University, Xi'an 710072, China)

Abstract: The rotor disk cavities of Marine gas turbine often cause self-excited vibrations due to fluid accumulation. The accumulated fluid forms by condensation of vaporized lubricating oil or water vapor. The rotor drives the liquid in the cavity to rotate, causing vibration instabilities. In this study, a horizontal flexible rotor system with two disks and two supports was examined experimentally. The rotor instability and stability restoration were observed, and the effects of the liquid volume and viscosity were studied to reveal the dynamic behaviors of small amounts of liquid in horizontal rotors. There was a threshold amount of liquid for the unstable vibrations, and instability occurred when the amount of fluid exceeded the threshold. A threshold speed of instability and recovery speed were found, both of which were higher than the critical speed. When the speed was higher than the threshold speed of instability, instability occurred. When the speed increased further, for speeds faster than the recovery speed, the instability disappeared. The amplitude of the total vibration increased suddenly, as did the sub-harmonic frequency. The fundamental and sub-harmonic frequencies were modulated and showed beat vibration characteristics. The threshold speed of instability decreased first and subsequently increased with the increase in fluid volume. With the increase in the viscosity coefficient of the fluid, the threshold speed of the fluid-filled rotor and amount of fluid increased. For unstable vibrations, the rate of amplitude growth increased rapidly.

Key words: Gas turbine rotor system; Unstable vibrations; Small amounts of fluid-filled; Threshold speed of instability; Threshold amount of liquid for the unstable vibrations

CLC number: V263.6 **Document code:** A **Article number:** 1001-4055 (2021) 09-2105-14

DOI: 10.13675/j.cnki.tjjs.200581

小积液情况下卧式转子的稳定性实验研究

王俨凯, 王彤, 廖明夫, 王鑫

(西北工业大学 动力与能源学院, 陕西 西安 710072)

摘要: 盘腔积液现象在舰用燃气轮机工作过程中时有发生, 汽化的滑油和水蒸汽凝结形成积液。转子带动腔内的积液旋转, 引发振动失稳, 严重时会对发动机结构造成致命性破坏。为此, 开展燃气轮机压气机盘腔积液的模拟实验研究, 以双盘双支承的卧式柔性转子系统作为研究对象, 重点关注小积液量的特点, 对积液转子的动力学稳定性进行了研究。观测到转子的失稳现象, 开展了不同积液体积、不同积液类型(水、植物油和滑油)等因素的影响规律研究, 揭示了小积液的卧式转子动力学特征。研究结果表明: (1) 对于积液失稳振动, 存在失稳边界积液量, 当积液量大于该边界值时, 失稳将会发生。

* 收稿日期: 2020-08-05; 修订日期: 2020-10-28。

基金项目: 国家科技重大专项(2017-I-0006-0007); 国家自然科学基金(51775436)。

通讯作者: 王俨凯, 博士, 副教授, 研究领域为发动机故障诊断。

引用格式: 王俨凯, 王彤, 廖明夫, 等. 小积液情况下卧式转子的稳定性实验研究[J]. 推进技术, 2021, 42(9):2105-2118. (WANG Yan-kai, WANG Tong, LIAO Ming-fu, et al. Experiment on Instability of Horizontal Rotor System Partially Filled with Small Amounts of Fluid[J]. *Journal of Propulsion Technology*, 2021, 42(9):2105-2118.)

(2) 失稳边界转速及恢复转速均高于临界转速。当转速高于失稳边界转速时,失稳将会发生。转速进一步增加,高于恢复转速时,失稳现象可能消失。(3) 失稳时的振动特征为:出现幅值突增,次谐波成分也随之增加;基频和次谐波发生调制,表现出拍振特征。(4) 随着积液体积的增加,失稳边界转速先减小后增加。(5) 随着积液粘度系数增大,失稳边界转速和边界积液量均增大。

关键词: 燃机转子系统;失稳振动;小积液量;失稳边界转速;失稳边界积液量

1 Introduction

In the working process of marine gas turbine, because of the condensation of vaporized lubricating oil or water vapor, liquid accumulation in the disk cavity often occurs. This phenomenon is one of the factors that causes the vibrations of the rotating machinery to exceed the standard. The oil that accumulates in the drum rotates with the rotor, and the free surface in the drum cavity can cause self-oscillation of the rotor. Firstly, such self-excited unstable vibrations often cause the vibrations of the whole rotor system to exceed the acceptable level. The vibrations subsequently cause secondary failures, such as frictional faults. Finally, this can cause fatal damage to the engine structure, with catastrophic consequences. In this study, the effects of parameters such as volume and viscosity of the fluid on the instability were investigated through experiments, which laid a foundation for further analysis of the fluid accumulation in the disc cavity.

There are two types of rotating machinery in which liquid accumulation in the disk cavity occurs. In the first type, which includes pumps, the working fluids or transport materials are liquid. There is often a large amount of liquid in the disk of cavity. To improve stability and reduce vibrations, a vertical rotor structure is generally used. The second type, which includes Marine gas turbine, often use horizontal rotor structures. Liquid accumulates in the cavity due to condensation of the lubricating oil or water vapor, and there is often only a small amount accumulated liquid. The presence of the liquid is not considered when designing the rotor. Therefore, the damage caused by oil accumulation in the disk cavity can be great. In this paper, the effects of oil accumulation on the dynamic stability of horizontal rotors are experimentally studied.

There have been few experimental studies on rotors with partially filled cavities. Zhu et al.^[1-3] carried out an

experiment with a vertical flexible rotor with a large amount of liquid in the cavity. In their studies, they examined the instability process of partially filled flexible rotor systems and the dynamic characteristics of the rotor system in the instability process. They also analyzed the influence of the quantity of liquid and fluid viscosity on the vibration and stability of rotor systems^[4]. Zhai et al.^[5] analyzed the leakage of lubricating oil in the drum cavity of aero-engines, and they analyzed the vibrations of the oil-accumulating rotor using simulations and experiments. The results showed that the instability of the oil-accumulating rotor was caused by the asynchronous self-excited vibration of the rotor system. The vibration characteristics of rotor instability were obtained. Zheng et al.^[6] analyzed the phenomenon of fluid accumulation in the drum cavity of an aero-engine. They determined that the asynchronous self-excited vibration was a sub-harmonic self-excited vibration, which led to the vibration of the rotor instability. Han et al.^[7] concluded that there were non-synchronous vortices between the fluid and the rotor when the speed of the fluid-filled rotor exceeded the first-order critical speed. They believed that the rotor system speed and the weight of fluid had a great influence on the non-synchronous amplitude and frequency. Zucht et al.^[8] conducted an experiment with a transparent horizontal cylinder with a large amount of liquid in the cavity. They analyzed the influence of gravity and the viscosity of the liquid and explored the distribution of the liquid in the cavity during rotation using a sectional scanner. Xu et al.^[9] used a single plate and double supported horizontal rotor in their experiments. They observed the distribution of different amounts of oil at different speeds using a high-speed camera. In Table 1, a comparison is made between the previous studies and this paper. The Fluid-filled ratio in this paper is different from previous studies.

The experimental research is gradually transitioning from vertical to horizontal rotors. Therefore, the in-

Table 1 Comparison of previous studies

	Literature	Tester device	Research content	Fluid-filled ratio	Key outcomes and requirements
Other rotating machinery	Zhu [1-3]	Vertical rotor	Single disc flexible rotor, cantilever structure	0.66~0.94	Relationship between a large amount of liquid and the threshold speed of instability are obtained.
	Zucht[8]	Horizontal cylinder		0.50	Oil distribution under different rotational speeds of large amount of liquid in cavity is observed.
Marine gas turbine	Zhai[5]	Horizontal rotor	Single disc flexible rotor with two supports	0.03, 0.05 (Two points)	Instability of the oil-accumulating rotor is a non-synchronous, self-excited vibration, but the influence of the amount of accumulated liquid was not examined.
	In this paper	Horizontal rotor	Double disc flexible rotor, supported at both ends	0.00~0.17 (Multi points simulation continuous)	For a small amount of fluid, the relationship between the threshold speed of the instability and the amount of fluid and between the instability vibration and the viscosity coefficient of fluid were obtained

Notes: the data of the winning bid * in the Table 1 are determined according to the estimated experimental parameters in the literature.

fluence of the liquid weight should be considered^[10]. Most of the previous studies did not focus on the small amount of fluid^[11-13]. However, in the working process of marine gas turbine, fluid accumulation in the disk cavity often occurs in small amounts^[14-18]. Through previous studies, the instability characteristics of the fluid-filled rotor in the disc cavity were obtained^[19]. However, to understand influence of the amount of liquid in the cavity on the instability of the rotor, the experiment should begin from the rotor without oil in the disk cavity, the oil quality should be increased gradually to describe the dynamic characteristics of the oil with different degrees comprehensively and determine the threshold speed and amount of oil in the disk cavity for instability to occur. To understand the influence of the viscosity of the liquid in the disc on the rotor dynamics, an experiment was carried out with three viscous liquids. The effects of the viscosity and volume of the liquid on the stability boundary are discussed. The effects of different factors on the unstable vibrations caused by liquid in the disc cavity are summarized, and the effects of the liquid on the critical speed of the rotor were analyzed.

Based on previous studies, the instability of a horizontal rotor partially filled with a small amount liquid at different fluid-filled ratios and viscosities was systematically studied. Firstly, the dynamic stability of horizontal rotors are explored, which were partially filled with liquid in the disc cavity. The relationship between the small amount of liquid in the disc cavity and the critical speed of the rotor are determined. Lastly, the effects of

three factors on the stability boundary are discussed: the viscosity of the liquid, the amount of liquid, and the acceleration and deceleration conditions.

2 Experimental scheme

2.1 Experiment on rotor partially filled with viscous liquid

2.1.1 Experimental device

To simulate liquid in the rotor disc cavity, the experimental device was a single-span, double-disk flexible horizontal rotor. Fig. 1 shows the rotor device.

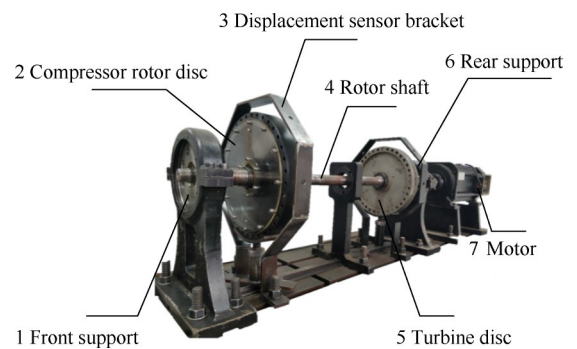


Fig. 1 Rotor device

In Fig. 1, labels 1 and 6 are the front and rear fulcrum of the rotor tester, both of which were rigid supports. The front fulcrum used a roller bearing, and the rear fulcrum used a deep groove ball bearing. Label 2 is the simulation disk of the liquid accumulation in the rotor cavity of the compressor, which was used to simulate the liquid phenomenon in the cylinder cavity of the compressor rotor. The size of the disc cavity was designed according to the cavity unit structure. Label 3 is the displacement

sensor bracket used to mount the sensor. Label 4 is the rotor shaft. Label 5 is the turbine simulation disc. Label 7 is the motor, which was controlled by the frequency conversion governor to provide power for the rotor system.

2.1.2 Rotating disk cavity

The disc cavity was consisted of two parts: the simulated disk and the simulated plate cover. The simulation plate was steel. The disk end face's inner and outer edges had seal slots to allow O-rings to be installed and prevent leakage of the liquid that filled the cavity.

To observe the flow characteristics of the liquid in the cavity during the experiment, a transparent acrylic material was used to fabricate the plate cover. A sealing ring was designed on the outer and inner edges of the plate cover, corresponding to the seal slot on the disk. A connecting hole was arranged on the inner and outer edges of the plate cover, which was solidly connected with the disk. In addition, two symmetrical through-holes were designed on the plate cover, which were used as the injection and draining holes. The holes were both 5 mm in diameter and were used to fill and drain the liquid.

The basic size of the disk is shown in Fig. 2. It was sealed by an O-ring and silicone seal pad.

During the experiment, the screw connecting the sealing part and the fluid-filled part was removed, and liquid was injected into the fluid-filled part. After adding the liquid, the sealing and the fluid-filled parts were reconnected, and the experiment was conducted. At the end of the experiment, the liquid was extracted and cleaned before carrying out other experiments. The fluid-filled ratio ranged from 0.00 to 0.17, that is, 0~

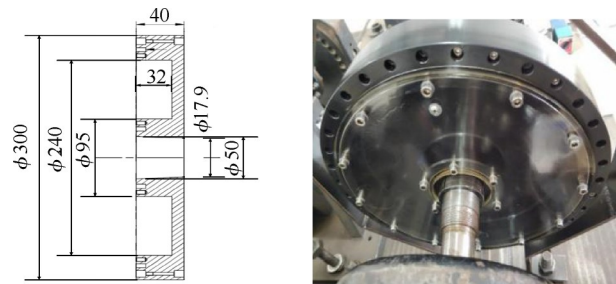


Fig. 2 Liquid charging device dimension diagram and photograph of the actual device (mm)

200 ml of liquid was added.

2.1.3 Vibration testing device

The schematic diagram of the tester and test system used in this experiment is shown in Fig. 3. The sensors of the test system mainly included an eddy current displacement sensor, electro-dynamic velocity sensor, and photoelectric sensor. They communicated with the data acquisition system, test software, signal transmission cable, computer, and other common components of the test system. The data measured by the sensor were processed by the data acquisition system, and the vibration data were collected, filtered, and amplified. After the analog/digital conversion, the data were sent to the computer, and the experimental data were analyzed and processed by the computer software.

Two displacement sensors were installed on the simulated compressor disk and the simulated turbine disc to measure the vibration displacement of the disc with liquid in the cavity. Two velocity sensors were vertically arranged at the front support of the simulated compressor, and the vibration velocity value at the bearing seat of the front support was measured along the direction of the front support to the motor. The information

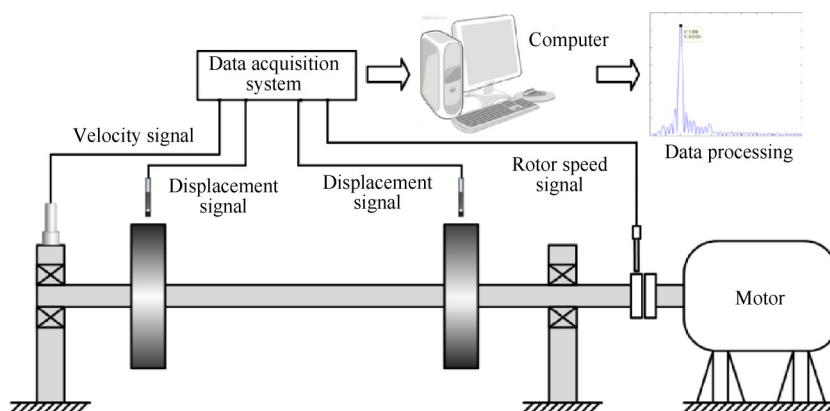


Fig. 3 Schematic diagram of the tester and test system

measured by each measuring point is shown in Table 2.

2.2 Experimental process

To study the influence of fluid accumulation in the disc cavity on the rotor vibrations, the effects of the fluid amount and viscosity coefficient were considered. The control variable method, and experiments were carried out by varying these two parameters.

During the experiment, different amounts of liquid were injected into the cavity through the injection hole to control the amount of liquid. The viscosity coefficient of the liquid was controlled by changing the type of liquid.

The experimental process was as follows:

(1) Amount of liquid

When changing the amount of liquid in the cavity, the sealing screw of the liquid injection hole on the plate cover was removed, and an appropriate amount of liquid was injected into the cavity through the liquid injection hole. The sealing screw was tightened after the injection was complete.

The total volume of the cavity was 1143.94 ml. The amount of liquid began at 0 ml, and the maximum amount of fluid-filled was 200 ml. The range of the fluid-filled ratio was 0~0.17.

The amount of liquid accumulated in the disc cavity of the rotor was unknown when the unstable vibrations began. To accurately determine the amount of liquid accumulated and improve the efficiency of the experiment, the amount of liquid accumulated began from 0 ml. Step sizes of 1, 2, 3, 5, 10, and 20 ml were used to increase the liquid volume.

Starting from 0 ml, a maximum volume of 20 ml was used to increase the amount of liquid. At the end of each group of experiments, the vibration data were ana-

lyzed to find the abnormal vibration peak caused by liquid in the cavity and the vibration component with large amplitude of sub-harmonic frequency. In the data analysis, if the signs of instability vibration caused by liquid in the cavity are observed, the adding step size of liquid will be shortened and the appropriate amount of liquid would be selected, until find the amount of liquid when the rotor is instable.

After finding the threshold amount of fluid at which unstable vibrations begin, a small amount of fluid near the threshold amount was selected to increase the volume and more accurately analyze the relationship between the vibration characteristics of the rotor and the instability threshold. The step size of additional liquid was gradually varied as needed to analyze the influence of the liquid on the vibration characteristics of the rotor.

(2) Viscosity coefficient of liquid

To control the viscosity coefficient of the liquid, the type of liquid injected into the cavity was varied. When filling with different types of liquids, the liquid viscosity, density, and other properties will be different. Three different types of liquids were used in the experiment, water, vegetable oil, and lubricating oil. The parameters of the three liquids are listed in Table 3.

By studying the influence of liquid viscosity on the vibrations of these three liquids, the influence of liquid viscosity on the rotor vibrations was summarized.

2.3 Dynamic performance of dry rotor

The dynamic characteristics of the rotor were verified by experiments after dynamic balancing. Running the rotor without fluid-filled, the speed increased slowly to 5200 r/min, after which it was decelerated. Fig. 4 is the amplitude-frequency characteristic diagram of the rotor. Since the natural frequency of the displacement

Table 2 Test channel information

Location and name of measuring point		Vibration information	Type	Sensitivity
Disk	Ch 1	Vertical displacement of compressor disc	B&K VIBRO IN-085	8mV/ μ m
	Ch 2	Horizontal displacement of compressor disc		
	Ch 3	Vertical displacement of turbine disc		
	Ch 4	Horizontal displacement of turbine disc		
Support	Ch 5	Vibration velocity of the front bearing 45° to the left	B&K VIBRO VS-080	75mV/(mm/s)
	Ch 6	Vibration velocity of the front bearing at 45° to the right		
Coupling	Photoelectric	Photoelectric information for rotor speed measurement	B&K VIBRO P-84/1	/

sensor bracket is 40Hz, the data starts from 2500r/min. In Fig.4, the solid line is the acceleration process, and the dotted line is the deceleration process. The peak at about 3200 r/min was the first order critical speed of the rotor. The first order critical speed during the acceleration process was 3237 r/min, and during the deceleration process it was 3231 r/min. The mean value of the first order critical speeds was 3234 r/min.

Table 3 Types and parameters of liquid

Type	Density/ (kg/m ³)	Viscosity/ (kg/(m·s))	Dynamic viscosity/ (m ² /s)
Water	1000	1.0 × 10 ⁻³	1.0 × 10 ⁻⁶
Vegetable oil	925	7.8 × 10 ⁻³	8.5 × 10 ⁻⁶
Lubricating oil	885	1.3 × 10 ⁻²	1.45 × 10 ⁻⁵

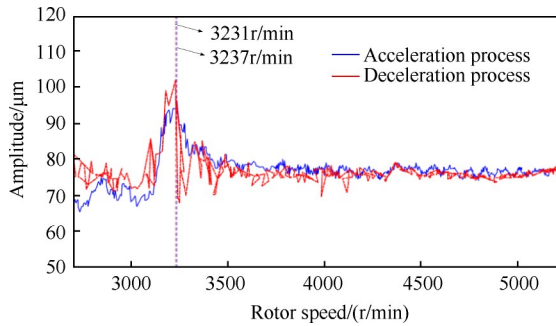


Fig. 4 Acceleration and deceleration process of rotor without liquid in the cavity

2.4 Dynamic characteristics of wet rotor

The experimental data were analyzed when the type of liquid in the cavity was water. The critical speeds for liquid amounts in the range of 0 ~ 200 ml were recorded

and summarized in Table 4.

By fitting the amount of liquid accumulated in Table 4 with the first order critical speed, the relationship between the first order critical speed with the amount of liquid accumulated was obtained, as shown in Fig. 5.

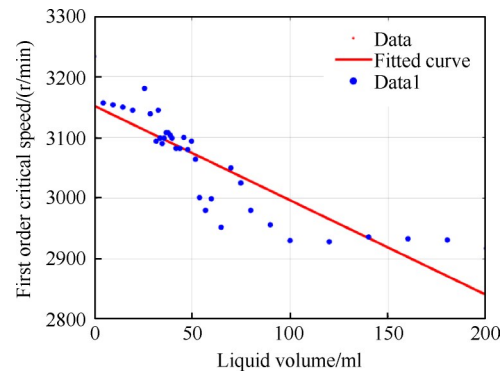


Fig. 5 Relationship between the first-order critical speed and the amount of liquid

As shown in the figure, compared with the rotor without liquid in the cavity, the critical speed of the rotor filled with 5 ml of liquid decreased by 87 r/min. Compared with the rotor filled with 5 ml of liquid, the critical speed of the rotor filled with 10 ml liquid decreased by 8 r/min. The presence of liquid in the disc cavity had a significant influence on the rotor critical features, but the increase in the amount of liquid had little effect on the rotor critical features. The reason may was that main factor affecting the rotor critical features was the fluid viscous force, and with the increase in the liquid volume, the influence of the viscous forces was greater

Table 4 Critical speed in the process of acceleration with different amounts of liquid

Amount of liquid/ ml	Critical speed/ (r/min)	Amount of liquid/ ml	Critical speed/ (r/min)	Amount of liquid/ ml	Critical speed/ (r/min)
0	3237	37	3108	60	2999
5	3150	38	3108	65	2952
10	3142	39	3104	70	3050
15	3152	40	3099	75	3025
20	3152	42	3082	80	2980
26	3096	44	3082	90	2956
29	3106	46	3100	100	2930
32	3090	48	3080	120	2928
33	3112	50	3094	140	2936
34	3093	52	3064	160	2933
35	3081	54	3001	180	2931
36	3099	57	2980	200	2917

than that of the gravitational force. In fact, the relationship between the first critical speed obtained from the experiments and the amount of liquid accumulated can be simply deduced.

The force of the liquid in the cavity on the rotor is as follows

$$F_1 = F_{lg} e^{j[(\Omega - \omega)t + \alpha]} + F_{lr} e^{j[(\Omega - \omega)t + \alpha + \frac{\pi}{2}]} \quad (1)$$

Where Ω is the rotor speed, ω is rotational speed of the fluid (namely axial vortex motion speed), and α is the bonding force of the initial phase angle. Thus, radial and tangential forces exist when fluid accumulates in a laminar flow state. Therefore, during operation, the liquid in the cavity has an influence on the rotor over a wide range of rotation speeds. In addition, the radial and tangential force frequencies of the liquid acting on the rotor are the same, with a phase difference of 90° . The force of the liquid on the rotor is inserted into the equation of motion. The radial force of disc is as follows

$$F_{lg} = \rho \Omega^2 \pi^2 LRh (R + \xi_{rotor}) + 2\rho g \pi^2 LRh \quad (2)$$

And the tangential force is:

$$F_{lr} = \frac{\rho^2 \Omega^3 \pi^2 LR^3 h}{2\mu} (R + \xi_{rotor}) \left(1 - \frac{\omega}{\Omega}\right) + \frac{\rho^2 g \pi^2 LRh}{2\mu} \left(\frac{R}{h} \Delta + \omega\right) (2R - h) \quad (3)$$

Where R is the rotor cavity diameter, L is the cavity width, μ is the viscous coefficient, h is the thickness of the liquid, ξ_{rotor} is the rotor eccentricity, and $\Delta = \Omega - \omega$.

The radial force of rotor F_ξ is as follows

$$F_\xi = F_{lg} + M\Omega^2 (\xi_{rotor} + \varepsilon) \quad (4)$$

Where M is the mass of the rotor system, ε is the eccentricity of disk. A radial force expression can be obtained by substituting it into the above equation:

$$\rho \Omega^2 \pi^2 LR^2 \left(\frac{h}{R}\right) (R + \xi_{rotor}) + 2\rho g \pi^2 LRh + M\Omega^2 (\xi_{rotor} + \varepsilon) = K\xi_{rotor} \quad (5)$$

K is the rotor stiffness coefficient. When $\omega_1 = \Omega$, the fluid-filled rotor vibrates unsteadily. In this case, equation (5) is

$$\rho \omega_1^2 \pi^2 LR^2 \left(\frac{h}{R}\right) (R + \xi_{rotor}) + 2\rho g \pi^2 LRh + M\omega_1^2 (\xi_{rotor} + \varepsilon) = K\xi_{rotor} \quad (6)$$

Where ω_1 is the rotational speed of the fluid-filled rotor along the rotor, namely the axial vortex velocity.

The above formula can be written as

$$\omega_1 = \sqrt{\frac{K\xi_{rotor} - 2\rho g \pi^2 LRh}{\rho \pi^2 LRh (R + \xi_{rotor} + \varepsilon) + M\xi_{rotor}}} \quad (7)$$

With $\omega_n^2 = K/M$, equation (7) can be written as

$$\omega_1 = \sqrt{\frac{M\xi_{rotor} \omega_n^2 - 2\rho g \pi^2 LRh}{\rho \pi^2 LRh (R + \xi_{rotor} + \varepsilon) + M\xi_{rotor}}} \quad (8)$$

When there was a small amount of liquid accumulated in the rotor disc cavity, the liquid surface thickness was very small. Thus, the latter term in the above equation is far smaller than the preceding one. If the formula $m_a = 2\pi RLh\rho$ for the mass of liquid accumulated is substituted into equation (8), the vibration speed is as follows

$$\omega_1 = \frac{\omega_n}{\sqrt{\frac{\pi m_a (R + \xi_{rotor} + \varepsilon)}{2M\xi_{rotor}} + 1}} < \omega_n \quad (9)$$

According to the above formula, $\omega_1 \approx \omega_n$, and $\omega_1 < \omega_n$. Therefore, the sub-harmonic frequency generated by the rotor under the action of liquid is lower than the natural frequency of the rotor without liquid. That is, the threshold speed of the unstable vibration of the fluid-filled rotor is above the first critical speed. Furthermore, the vibration speed ω_1 of the fluid-filled rotor decreases with an increase in the amount of liquid.

3 Experimental results on unstable vibrations

3.1 Description of instability phenomena

Fig. 6 shows the vibration amplitude of each channel versus the rotor speed when the cavity was filled with 35 ml of water. The upper half of the figure shows the variation of rotor speed with time. As shown in the figure, the speed increased slowly from 2700 to 5200 r/min, after which it gradually slowed to 2700 r/min. The bottom half shows the vibration amplitude variation with time.

During the acceleration process, when the rotor speed increased to the first order critical speed of 3099 r/min, the rotor vibration exhibited an obvious peak. After passing the first critical speed, the vibration amplitude of the rotor decreased. However, another vibration peak appeared when the speed increased to 3300 r/min, which was significantly higher than the vibration peak at

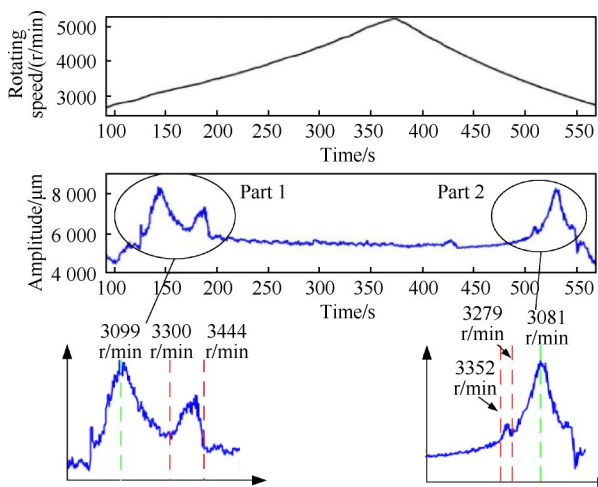


Fig. 6 Vibration analysis when cavity was filled with 35 ml of water

the first critical speed. The peak vibration was caused by liquid accumulation, and it disappeared after the rotor speed increased to 3444 r/min. As the rotor speed continued to increase to 5200 r/min, the rotor vibration was in a stable state, and no abnormal vibration peaks appeared.

After the rotor speed reached 5200 r/min, it was decelerated. When the rotor decelerated to 3352 r/min, a rotor vibration peak appeared, and the peak vibration disappeared at 3279 r/min. When the speed continued to decelerate to 3081 r/min, the rotor crossed the first-order critical speed and exhibited an obvious peak vibration. The rotor then decelerated to a stop.

When the rotor cavity was filled with 35 ml of water, the instable recovery boundary in the acceleration process was 3444 r/min, and the upper boundary speed in the deceleration process is 3352 r/min. The instable recovery boundary speed in the acceleration process of the rotor was greater than the upper boundary speed in

the deceleration process.

The vibration data of these experiments were analyzed, and the vibration order diagram of each channel was drawn, as shown in Fig. 7. As shown by the spectrum analysis, the rotor vibration was mainly before 2X, so the range of the axis was 0 to 3X.

In the displacement signal, there were mainly 1X components within the range of rotor speeds, and a relatively obvious 0.94X harmonic component appeared near 3400 r/min. As shown in Fig. 7, the vibration information collected by CH1 and CH2 channels was basically consistent.

3.2 Characteristics of unstable vibrations

When the cavity was filled with 36 ml of water, Fig. 8 shows the vibration amplitude of rotor CH1.

When the rotor speed increased to the first critical speed of 3099 r/min, the rotor vibration peaked. After passing the first critical speed, the rotor vibration decreased. However, when the rotor speed increased to 3303 r/min, the vibration amplitude of the rotor increased abruptly. As the speed increased, the vibration amplitude increased rapidly, exceeding the measurement range of the sensor. Meanwhile, the rotor vibrations were accompanied by an abnormal sound. After the emergency deceleration, the rotor vibration returned to normal.

The spectrum variation within the instability range after the rotation speed of 3303 r/min was analyzed, as shown in Fig. 9. With the increase in the rotor speed, the frequency band of the sub-harmonic became wider.

After the rotor speed reached 3303 r/min, the fluid-filled rotor generated a sub-harmonic frequency. As the rotor speed increased gradually, the sub-harmonic

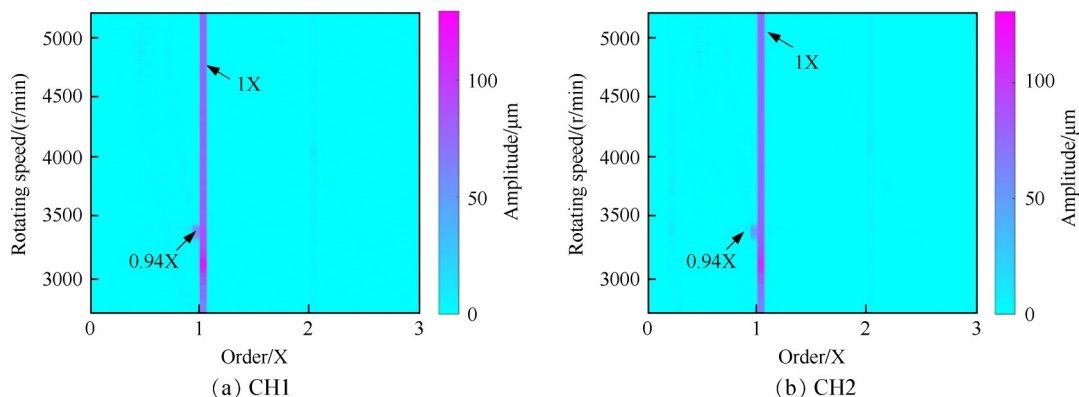


Fig. 7 Vibration orders for 35 ml of water

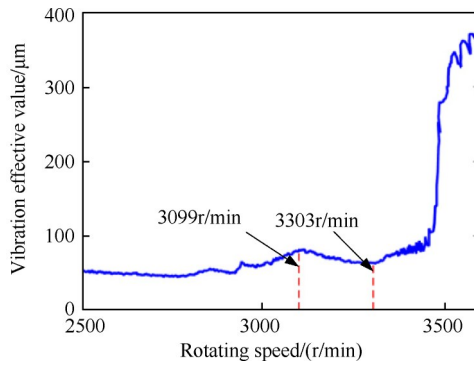


Fig. 8 Vibration monitoring for cavity filled with 36 ml of water

frequency band became wider gradually, from 0.94X to 0.81X, and the range of sub-harmonic frequency band was 48.5 to 56.3Hz. The amplitude dominant frequency also developed from 0.94X to 0.88X, and the amplitude of unstable vibrations was much larger than that of rotor 1X.

Fig. 10 shows the variation of the rotor sub-harmonic amplitude with rotor speed when the cavity was filled with 36 ml of water.

As shown in Fig. 10, when the rotor speed reached about 3300 r/min, the amplitude of the sub-harmonic frequency exhibited a rapid increase, reaching a maximum of 500 μm, and it still showed an upward trend.

Fig. 11 shows the variation in the amplitude of the fluid-filled rotor 1X with rotor speed when it was filled with 36 ml water. When the rotor exceeded the first-or-

der critical value, the amplitude of the 1X vibration increased significantly. After passing the first critical speed, the 1X amplitude of the rotor began to decrease. However, at about 3400 r/min, as the rotor entered a state of instability, and the 1X frequency amplitude also showed obvious fluctuations.

The time-domain waveform shows that the rotor vibration amplitude increased. With the increase in rotation speed, the beat vibration amplitude continued to increase. The fluid-filled rotor exhibited several characteristics when it produced unstable vibrations, and the following identification criteria were established:

(1) After the rotor passed the first-order critical speed, the instable state of the fluid-filled rotor caused a sudden increase in the vibration amplitude.

(2) When the fluid-filled rotor entered the instable state, the sub-harmonic component of the rotor vibrations within the range of 0.5X~1X increased abruptly.

(3) When the fluid-filled rotor entered the instable state, the time-domain waveform of rotor vibrations exhibited a beating phenomenon, and the amplitude of the 1X of the rotor fluctuated.

4 Effects of different factors on stability

4.1 Influences of liquid accumulation on instability threshold speed

To analyze the influence of the amount of liquid on

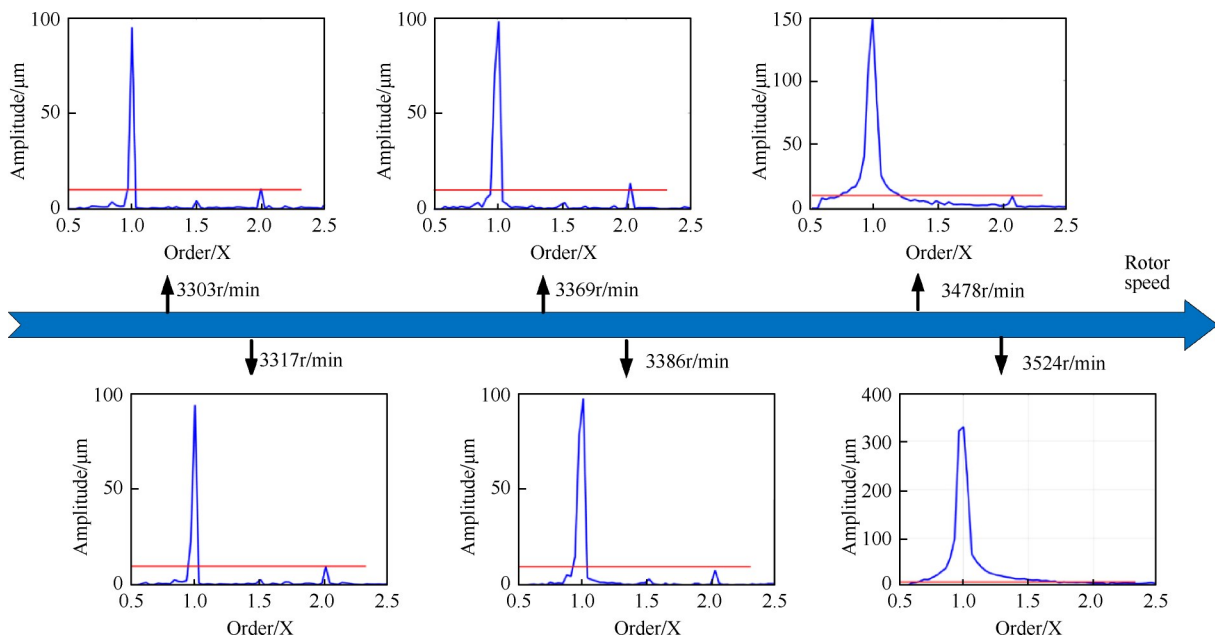


Fig. 9 Spectrum variation analysis with rotor speed

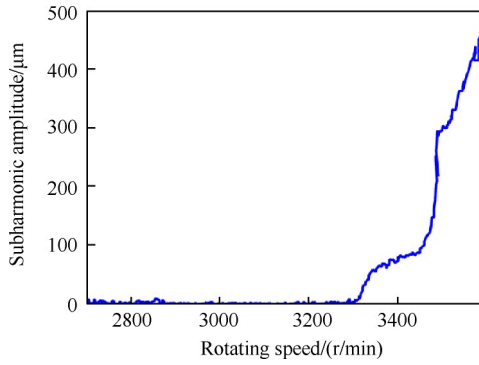


Fig. 10 Sub-harmonic amplitude

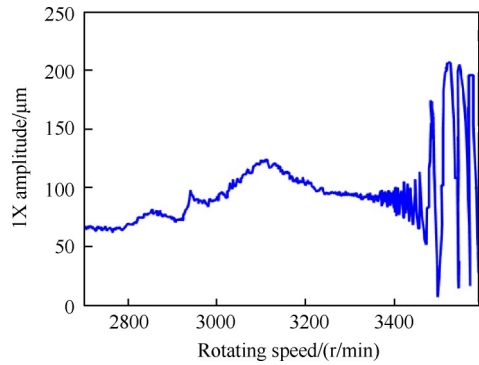


Fig. 11 1X amplitude

the threshold speed of instability, the instability vibration data with liquid volumes greater than 35 ml were analyzed. For water, the vibration data from 35 to 200 ml were used to analyze the unstable threshold speed and the first critical speed of each group of data. The threshold speed of instability was determined as the rotor speed at which the sub-harmonic amplitude of the vibrations was greater than $10 \mu\text{m}$. The first order critical speed was determined by taking the speed at the maximum amplitude of 1X when the rotor passed the first order critical value. The ratio of the threshold speed to the first critical speed was also calculated.

Fig. 12 shows the relationship between the threshold speed of the fluid-filled rotor and the amount of liquid.

Based on the fitting results, there was not a simple positive correlation between the threshold speed of instability and the amount of accumulated liquid, but with the increase in the amount of liquid, the threshold speed of instability first decreased and then gradually increased. However, the minimum value of the threshold speed of instability was not lower than the first critical speed of the rotor.

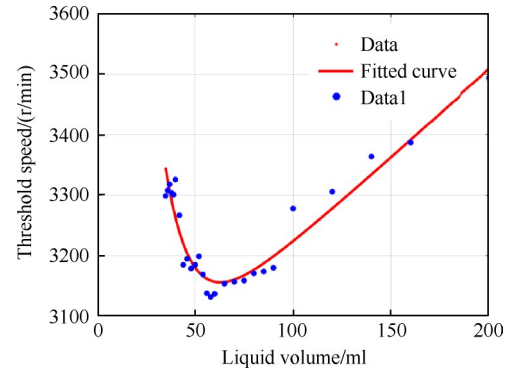


Fig. 12 Relationship between threshold speed of instability and amount of accumulated liquid

The relationship between the instability threshold speed obtained from the above experiments, and the amount of liquid accumulated can be simply deduced. The motion equation of the rotor was established as follows

$$M \ddot{r} + D \dot{r} + Kr = M(\xi_{\text{rotor}} + \varepsilon)\Omega^2 + Mg \sin\delta + F_{1\xi} \quad (10)$$

D is the rotor damping ratio. It can be deduced from equation (9) that the vibrations of the rotor under the action of liquid accumulation were in the sub-harmonic resonance frequency band. That is, the threshold speed of the unstable vibrations of the rotor was about above the first critical speed. The factor causing the unstable vibration of the rotor was the effect of liquid accumulation on the rotor force. To highlight the main characteristics of the unstable vibrations and simplify the calculation process, the cross stiffness term k_{xy} caused by liquid in the cavity force was introduced, and the above equation can be written as follows

$$M \ddot{r} + D \dot{r} + (K - jk_{xy})r = 0 \quad (11)$$

From this solution, the characteristic equation can be derived

$$Ms^2 + Ds + K - jk_{xy} = 0 \quad (12)$$

s is the characteristic root of the characteristic equation. And the expression of the instability speed obtained is as follows

$$\Omega_{\text{instability}} = \sqrt[6]{\frac{64\nu^2 D^2 K^2 M}{\pi^2 R^4 m_c^2 (1 - \gamma)^2}} \quad (13)$$

Where $\nu = \mu/\rho$ is the liquid dynamic viscosity, D is the rotor damping ratio, and $\gamma = \omega/\Omega \in [0.5, 1)$. $\Omega_{\text{instability}}$ is the lower boundary of the instability interval. According to equation (13), the threshold speed of the insta-

ble hydro-static rotor is mainly affected by the rotor structure parameters. The instability threshold speed ratio of the fluid-filled rotor $\eta_{instability}$ is

$$\eta_{instability} = \frac{\Omega_{instability}}{\omega_1} = \sqrt[6]{\frac{64v^2 D^2 K^2 M}{\pi^2 R^4 \omega_n^6 (1-\gamma)^2 m_c^2} \left[\frac{\pi(R + \xi_{rotor} + \varepsilon)}{2M\xi_{rotor}} m_c + 1 \right]^3}$$

(14)

Considering the same fluid-filled rotor, the main factors affecting the instability boundary $\eta_{instability}$ can be written as

$$\eta_{instability} = K_2 \sqrt[6]{\frac{(K_1 m_c + 1)^3}{m_c^2}}$$

(15)

Where $K_1 = \frac{\pi(R + \xi_{rotor} + \varepsilon)}{2M\xi_{rotor}}$

$$K_2 = \sqrt[6]{\frac{64v^2 D^2 K^2 M}{\pi^2 R^4 \omega_n^6 (1-\gamma)^2}}$$

Since m_c is the amount of liquid in the cavity. The relationship between the threshold speed of instability and the amount of accumulated liquid was as follows in Table 5.

When the $m_c \in \left(0, \frac{4M\xi_{rotor}}{\pi(R + \xi_{rotor} + \varepsilon)}\right)$ and the

amount of liquid accumulated increases, the threshold speed ratio of instability $\eta_{instability}$ decreases.

When the $m_c \in \left(\frac{4M\xi_{rotor}}{\pi(R + \xi_{rotor} + \varepsilon)}, +\infty\right)$ and the

amount of liquid accumulated increases, the threshold speed ratio of instability $\eta_{instability}$ increases.

When the $m_c = \frac{4M\xi_{rotor}}{\pi(R + \xi_{rotor} + \varepsilon)}$, the threshold

speed ratio of $\eta_{instability}$ is the minimum value, but its value is greater than 1.

Therefore, with the increase in the amount of liquid, the threshold speed of instability $\eta_{instability}$ will decrease and then increase. The existence of the extreme point is unavoidable because of the deflection of the flexible rotor ξ_{rotor} . If the deflection of the flexible rotor is not considered, the extreme point will not exist.

Based on the above theoretical analysis and experimental results, there is an inflection point between the threshold speed of instability and the amount of accumulated liquid when the fluid-filled ratio is between 0 and 0.08, which was not found in previous experimental studies. It can also be seen from Table 1 that the fluid-filled ratio range at this inflection point was just inside the fluid-filled ratio range of marine gas turbine cavities. The discovery of this characteristic is of great significance for the design of oil rejection holes and the diagnosis of fluid accumulation in marine gas turbine.

4.2 Influence of liquid viscosity on instability threshold speed

In this experiment, when water was added into the rotor disc cavity gradually, the instability was detected at 35 ml. When the liquid was vegetable oil, the instability was observed at 98 ml. Finally, when the liquid was lubricating oil, the instability was observed at 200 ml. The amount of liquid at which the first unstable vibration of the fluid-filled rotor occurs is called the amount of liquid at the instable threshold.

The vibration data of the cavity filled with 35 ml of water, 98 ml of vegetable oil, and 200 ml of lubricating oil were analyzed, as shown in Fig. 13.

The threshold speed of the above three groups of experimental data was determined according to the instable state identification criteria presented in Section 3.2. The instable threshold speed and liquid amount of the fluid-filled rotor under the three types of liquid were calculated and are summarized in Table 6.

Table 5 $\eta_{instability}$ addition and subtraction analysis

Parameter	Range and trend of change					
m_c	$\left(-\infty, -\frac{1}{K_1}\right)$	$-\frac{1}{K_1}$	$\left(-\frac{1}{K_1}, 0\right)$	$\left(0, \frac{2}{K_1}\right)$	$\frac{2}{K_1}$	$\left(\frac{2}{K_1}, +\infty\right)$
$\eta_{instability}(m_c)$	+	0	-	-	0	+
$\eta_{instability}$	Increase	Maximum points	Decrease	Decrease	Minimum points	Increase

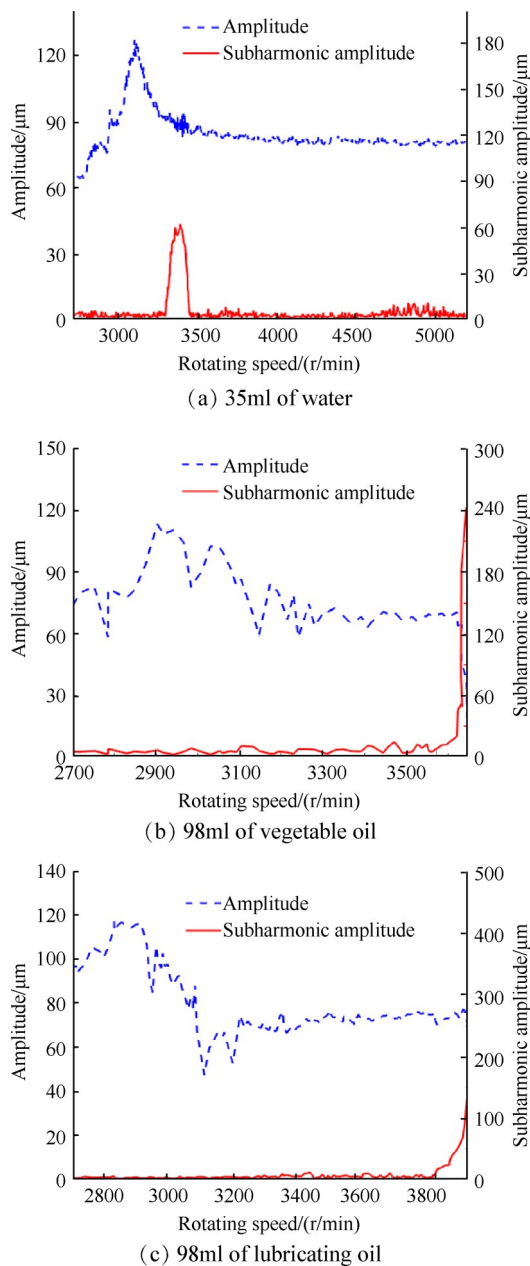


Fig. 13 Relationship between 1X amplitude and sub-harmonic amplitude of different types of liquids

From Table 6, it can be seen that: With the in-

crease in the viscosity coefficient of the liquid, the threshold speed of instability of the fluid-filled rotor increased accordingly.

With the increase in the viscosity coefficient of the liquid, the instability threshold liquid amount of the fluid-filled rotor exhibited an upward trend.

The vibration intensities of the fluid-filled rotors were different for the three types of liquids with different viscosity coefficients. The vibration data for 36 ml of water, 98 ml of vegetable oil, and 200 ml of lubricating oil were analyzed.

Based on the analysis of the characteristics of the unstable vibration in Section 3.2, the sudden increase in the amplitude during the unstable vibrations of the fluid-filled rotor was caused by the vibration component of the sub-harmonic frequency. Therefore, the relationship between the amplitude of the sub-harmonic frequency and rotation speed of three groups of experimental data were plotted, as shown in Fig. 14~16.

Compared with the analysis results of the three groups of data, the amplitude growth rate of the unstable vibrations was different for different viscosity coefficients. Therefore, the rotor speed and corresponding sub-harmonic amplitude with different viscous coefficients after the sudden increase were counted, as shown in Table 7.

The slope of the amplitude growth rate was used to indicate the speed of the amplitude increase. The slope of amplitude growth rate of different types of liquid was obtained by fitting, as shown in Table 8.

The influence of viscosity coefficient on the slope of amplitude growth rate was obtained, as summarized in Table 8. When the unstable vibration was caused by

Table 6 Instability threshold speed and liquid amounts for different types of liquids

Type	Viscosity coefficient/(m ² /s)	Instability threshold speed/(r/min)	Instability threshold liquid amount/ml
Water	1.0 × 10 ⁻⁶	3300	35
Vegetable oil	8.5 × 10 ⁻⁶	3596	98
Lubricating oil	1.45 × 10 ⁻⁵	3841	200

Table 7 Sub-harmonic amplitude of each rotor speed for different types of liquids

Liquid type	Water			Vegetable oil			Lubricating oil		
Rotor speed/(r/min)	3402	3481	3555	3624	3632	3645	3921	3926	3934
Rotor-speed increment/(r/min)	0	79	153	0	8	21	0	5	13
Sub-harmonic amplitude/μm	81.38	177.40	395.60	45.92	182.80	242.90	69.81	90.77	430.60

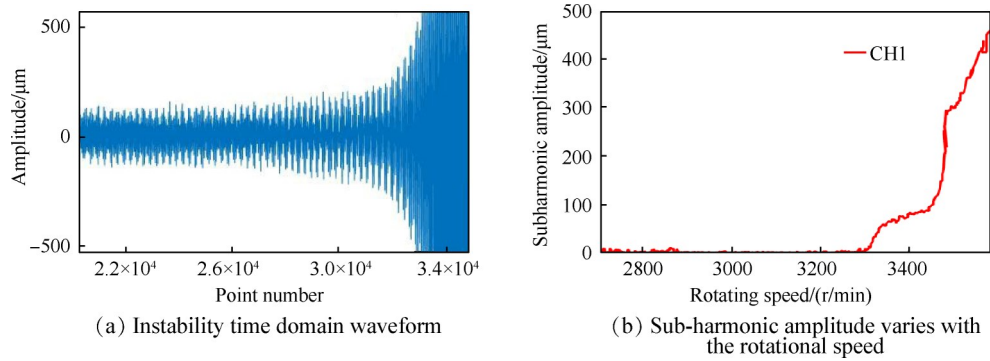


Fig. 14 Cavity filled with 36 ml water

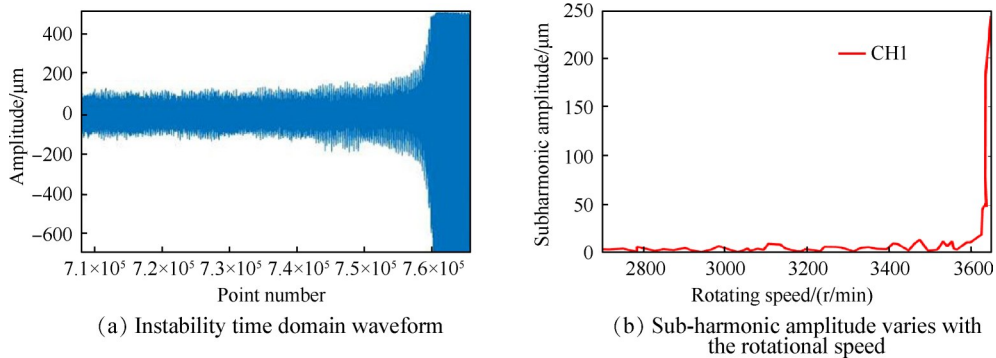


Fig. 15 Cavity filled with 98 ml vegetable oil

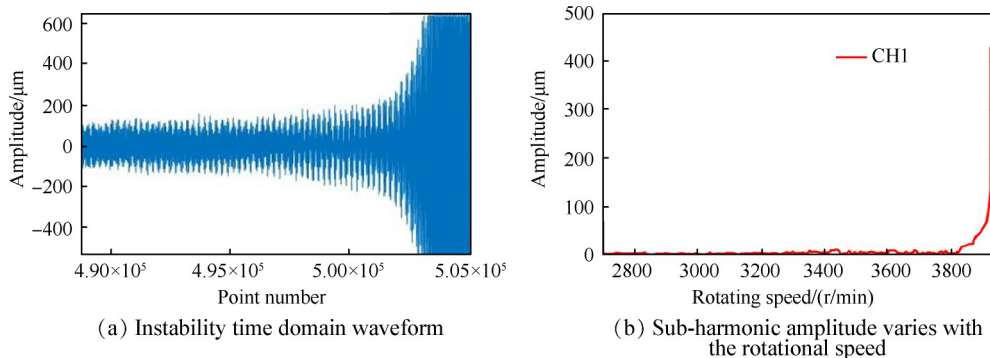


Fig. 16 Cavity filled with 200 ml lubricating oil

Table 8 Viscosity coefficient and slope of amplitude growth rate

Type	Water	Vegetable oil	Lubricating oil
Viscosity coefficient/(kg/(m·s))	1.0×10^{-3}	7.8×10^{-3}	1.3×10^{-2}
Slope of amplitude growth rate	2.04	8.92	29.12

fluid accumulation in the rotor disc cavity, with the increase in the viscosity coefficient of fluid accumulation, the amplitude and slope of the amplitude increase in the unstable vibrations of the rotor increased significantly.

5 Conclusions

The following results were obtained:

(1) There was an instability threshold of the liquid volume. In our experiment, the instability threshold liquid volume was 35 ml. If the liquid was less than 35 ml, the rotor system did not become unstable.

(2) The rotor's self-excited unstable vibrations appeared after the first critical speed. The total vibration amplitude increased, the sub-harmonic amplitude increased, and a beat vibration appeared.

(3) With the increase in the viscosity coefficient of the fluid in the rotor disc cavity, the instability threshold speed of the rotor and the instability threshold fluid volume increased.

The innovation of this study lies in many experiments. Furthermore, the inflection point as the amount of liquid increased was found first, which expanded the range of the relationship between the amount of liquid and the instability threshold speed curve. Instable experiments for the liquid in a cavity with different viscosity coefficients were carried out, and the effects of fluid viscosity on the vibration characteristics of rotor instability were determined, which are references for the fault diagnosis of gas turbine.

The shortcomings of this study were as follows. In the experiments of the unstable vibrations of the rotor partly filled with liquid, the amount of fluid in the disc cavity was small. Thus, the thickness of the liquid film was thin. As the rotation speed increased, the transition from laminar to turbulent flow could be observed easily. Thus, it is important to improve the method of observation. The advanced method of observation could be used to determine the distribution state of fluid in the disc cavity at different rotating speeds and reveal the mechanism of rotor unstable vibrations caused by fluid in the disc cavity.

Acknowledgments: The research was supported by the National Science and Technology Major Project and National Natural Science Foundation of China.

Reference

- [1] 祝长生. 部分充液悬臂柔性转子系统不稳定特性的实验研究[J]. 振动工程学报, 2003, 12, 16(4): 453-456.
- [2] 祝长生. 支承刚度各向异性部分充液转子系统的稳定性[J]. 航空动力学报, 2000, 15(4): 432-434.
- [3] Zhu Changsheng. Experimental Investigation into the Instability of an Over-Hung Rigid Centrifuge Rotor Partially Filled with Fluid[J]. *Journal of Vibration & Acoustics*, 2002, 128(3): 392-401.
- [4] Zhu Changsheng. Effect of Fluid Viscosity on Stability of a Flexible Rotor Partially Filled with Fluid[J]. *Journal of Zhejiang University (Engineering Science)*, 2004, 38(4): 484-489.
- [5] Zhai Jingyu, Zhang Hao, Han Qingkai, et al. Modeling and Experiments of Rotor System with Oil-Block Inside Its Drum Cavity[J]. *Journal of Vibroengineering*, 2013, 15(4): 1972-1982.
- [6] 郑旭东, 张连祥. 航空发动机整机振动典型故障分析[J]. 航空发动机, 2013, 39(1): 34-37.
- [7] Han Q, Wang M, Chu H. Nonsynchronous Vibrations of Rotor System with an Oil-Block Inside the Rotating Drum [J]. *Advances in Vibration Engineering*, 2013, 12(2): 165-178.
- [8] Zucht A. Investigation of the Phase Interface of a Fluid Dynamical System with Experimental and Numerical Methods [J]. *Forschung Im Ingenieurwesen Engineering Research*, 2008, 72(4): 241-258.
- [9] 许涛. 单盘积油转子系统动力学特性研究[D]. 大连: 大连理工大学, 2015.
- [10] 王俨割, 廖明夫, 丁小飞. 航空发动机故障诊断[M]. 北京: 科学出版社, 2020
- [11] 王鑫. 部分充液转子的理论与实验研究[D]. 西安: 西北工业大学, 2019
- [12] Kern D, Jehle G. Dynamics of a Rotor Partially Filled with a Viscous Incompressible Fluid[J]. *Pamm*, 2016, 16(1): 279-280.
- [13] 金业壮, 韩清凯, 闻邦椿. 积油转子系统的仿真[J]. 中国工程机械学报, 2015, 13(2): 109-113.
- [14] 王光定. 基于三维流动分析的充液转子动力稳定性研究[C]. 南京: 第十二届全国振动理论及应用学术会议论文集, 中国振动工程学会, 2017.
- [15] 刘杰, 黄文伟, 黄步玉. 部分充液转子系统的异步振动[J]. 上海交通大学学报, 1991(1): 1-9.
- [16] Rietz M, Scheid B, Gallaire F, et al. Dynamics of Falling Films on the Outside of a Vertical Rotating Cylinder: Waves, Rivulets and Dripping Transitions[J]. *Journal of Fluid Mechanics*, 2017, 832: 189-211.
- [17] Kozlova A N, Kozlov N V. Dynamics of Immiscible Liquids in a Rotating Horizontal Cylinder[J]. *Physics of Fluids*, 2016, 28(11).
- [18] Akerstedt H O, Jansson I. The Stability of a Flexibly Mounted Rotating Cylinder in Turbulent Annular Fluid Flow [J]. *Journal of Fluids and Structures*, 2015, 58(2): 152-172.
- [19] Kozlov N V. Effect of Vibration on Two-Liquid System in Rotating Cylinder [J]. *Acta Astronautica*, 2016: 561-571.

(编辑:刘萝威)